Available online at www.sciencedirect.com
ScienceDirect
Applied Surface Science 253 (2007) 3678–3682
applied surface science
www.elsevier.com/locate/apsusc

Effect of nano-titanium hydride on formation of multi-nanoporous TiO_2 film on Ti

Yung-Hsun Shih [a,b], Che-Tong Lin [b,c], Chung-Ming Liu [d], Chang-Chih Chen [b,e], Chin-Sung Chen [f,g], Keng-Liang Ou [c,*]

[a] *Dental Department of Wan-Fang Hospital, Taipei Medical University, Taipei 110, Taiwan*
[b] *School of Dentistry, College of Oral Medicine, Taipei Medical University, Taipei 110, Taiwan*
[c] *Graduate Institute of Oral Sciences, College of Oral Medicine, Taipei Medical University, Taipei 110, Taiwan*
[d] *Department of Chemical and Material Engineering, Lunghwa University of Science and Technology, Taoyuan 33306, Taiwan*
[e] *Department of Emergency Medicine, Mackay Memorial Hospital, Taipei 110, Taiwan*
[f] *Department of Dentistry, Cathay General Hospital, Taipei 110, Taiwan*
[g] *Department of Dentistry, Cathay General Hospital, Sijhih, Taipei 110, Taiwan*

Received 12 May 2006; received in revised form 29 July 2006; accepted 29 July 2006
Available online 12 September 2006

Abstract

The effect of titanium hydride on the formation of nanoporous TiO_2 on Ti during anodization has been investigated by X-ray photoelectron spectroscopy, grazing incident X-ray diffraction, transmission electron microscopy and scanning electron microscopy. Titanium hydride (TiH_2) was formed after cathodization, profoundly impacting the formation of nanoporous TiO_2 on Ti by anodization. Oxide layer and nanocrystal structure were observed after anodization with cathodic pretreatments. A multi-nanoporous TiO_2 layer was formed on the titanium. The titanium hydride is a nanostructure. The nanostructure is directly changed to nanoporous TiO_2 by a dissolution reaction during anodization. The nanoporous layer is difficult to form without cathodization. The nanostructural TiH_2 is important in forming a nanoporous TiO_2 layer. Anodization treatment with cathodic pretreatment not only yields a titanium surface with a multi-nanostructure, but also transforms the titanium surface into a nanostructured titanium oxide surface.

Keywords: Titanium; Implant; Nanoporous; Titanium oxide film

1. Introduction

Titanium and its alloys have been widely applied in dental and orthopedic implants such as prostheses used as joint replacements, because they have excellent biocompatibility, superior mechanical strength and high corrosion resistance [1–3]. Though commercially titanium-based implants with native oxide films have been long-term clinical success, enhancement of integration between bone and an implant may still be expected in clinical application. Various approaches have been utilized to increase the surface roughness of implants and thus promote bone–tissue integration [6–18]. Topographic characteristics of implants range from millimeters to nanometers are believed to affect the biological response of the host [4,5]. Titanium-based implants with porous layers induced bony ingrowth into the porous structure [6]. As mentioned above, the porous structure is able to improve bone integration. However, the porous oxide layer on Ti cannot easily be produced in the absence of a TiH_2 layer during immersion in alkaline solutions. The formation of porous TiO_2 on Ti has also been confirmed by presence of TiH_2 as a critical factor [7,8]. However, porous TiO_2 was prepared by immersing Ti in an alkaline solution for a long period. In the present study, hydrogen and oxygen was incorporated into Ti by cathodization before anodizing. Additionally, nanoporous TiO_2 was formed by submerging hydrogen-charged Ti in an alkaline solution for a short period. Titanium with nanoporosity and high biocompatibility was developed and investigated clearly. Hydrogen charging has been used to pretreat the Ti surface. However, it is no evident that the formation of nanoporous layer is related with nanostructure with electrochemical pretreatments [7,8]. This

* Corresponding author. Tel.: +886 2 27361661x5128; fax: +886 2 27362295.
E-mail address: klou@tmu.edu.tw (K.-L. Ou).

0169-4332/$ – see front matter © 2006 Elsevier B.V. All rights reserved.
doi:10.1016/j.apsusc.2006.07.081

study investigates exactly how titanium hydride affects the formation of nanoporous TiO_2 on Ti during anodization by X-ray photoelectron spectroscopy, grazing incident X-ray diffraction, transmission electron microscopy and scanning electron microscopy. Specimens are evaluated by electrochemical measurements and material analyses to elucidate the microstructure and surface properties of Ti with and without electrochemical treatments.

2. Experimental procedure

The substrate was a Grade II CP-Ti sheet. The Ti was cut into sheets with a diameter of 14.5 mm and a thickness of 1 mm (BioTech One Inc., Taipei, Taiwan). The specimens were mechanically polished using 1500 grit paper and further polished using diamond abrasives through 1 μm. The specimens were finished with colloidal silica abrasives through 0.04 μm. All specimens were degreased and pre-pickled in acid by washing in acetone, processing in through 2% ammonium fluoride, a solution of 2% hydrofluoric acid and 10% nitric acid at room temperature for 60 s. Finally, the specimens were etched in an aqueous mixture of HF (2 vol%) and HNO_3 (4 vol%) at room temperature for several seconds, and then washed in distilled water in an ultrasonic cleaner. Subsequently, titanium underwent cathodic polarization at a constant current for 10 min in 1 M H_2SO_4 solution at 298 K. The cathodic charging current density was kept from 0.1 to 5 A/cm^2. A platinum plate was used as a counter electrode in this process. Chemically etched titanium was treated by anodization at a constant current of 15 A/cm^2 for 10 min in 5 M NaOH solution to form a multi-nanoporous TiO_2 layer on the titanium surface. The specimens with and without anodization were compared with the specimens that had undergone cathodization before anodizing. The variations in the phase transformation and the microstructure were observed by transmission electron microscopy (TEM) and grazing angle X-ray diffractometry (GIXRD). X-ray photoelectron spectroscopy (XPS) was conducted to determine the chemical states and the oxide thickness. Depth profiles of oxide thickness were performed by continuous sputter etching with 3 keV Ar ion. Measuring area was at a diameter of 2 μm × 4 μm. For the determination of the oxide thickness, the relation $d = v_o t_d$, where d is the film thickness, v_o the sputtering rate and t_d the sputtering time when the oxygen peak amplitude at the metal-oxide interface has decreased to 50% of its steady state value in the oxide. To be precise, calibration of the sputtering rate was double-checked by two reference materials of 92 nm of TiO_2 and 100 nm of SiO_2. The reference TiO_2 film was deposited on (1 0 0) Si by RF sputtering system. By using Ellipsometry, the reference TiO_2 film was characterized as 92 nm in the oxide thickness and 2.2 in the refractive index with the values between 2.0 for amorphous type and 2.5 for anatase type of TiO_2 crystal structure. With the quoted two reference materials, the sputtering rate is about 0.1 nm/s. To assess the experimental standard deviation of the oxide thickness measured in the present study, the depth profile was performed on the randomly selected three specimens before and after treatments. The multi-nanoporous Ti surfaces were determined by scanning electron microscopy (SEM).

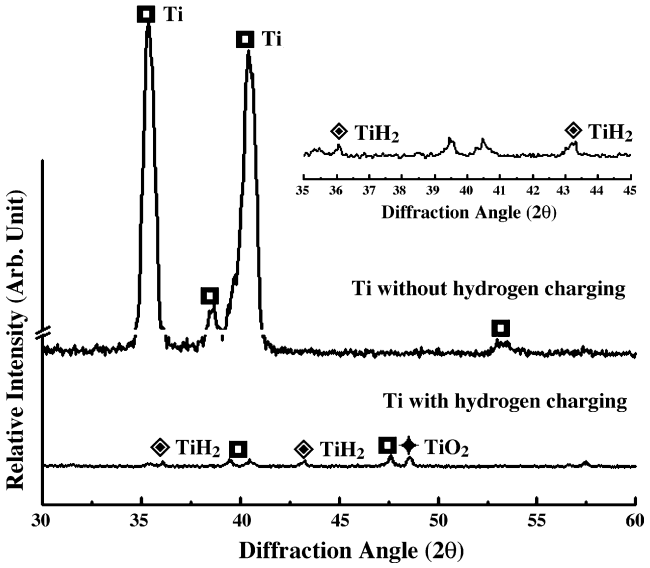

Fig. 1. XRD spectra of Ti with and without cathodic pretreatment.

3. Results and discussion

Fig. 1 displays GIXRD spectra of titanium with and without hydrogen charging. For Ti without hydrogen charging, only reflections of Ti peaks are observed and the structure is crystalline. Moreover, numerous reflection peaks, excluding Ti peaks, are obtained from Ti with cathodic polarization. The crystalline structure of hydrogen-charged Ti comprises Ti and TiH_2 phases, similar to that reported by Tanaka et al. [7,8].

Fig. 2 presents TEM micrographs and selected area diffraction patterns (SADP) of Ti with cathodization. The figure shows a bright-field electron micrograph of the cathodized Ti, which was taken from the titanium matrix in the [0 0 1] zone. The figure indicates the presence of a crystalline hcp structure in the Ti matrix. Fig. 2 also displays an

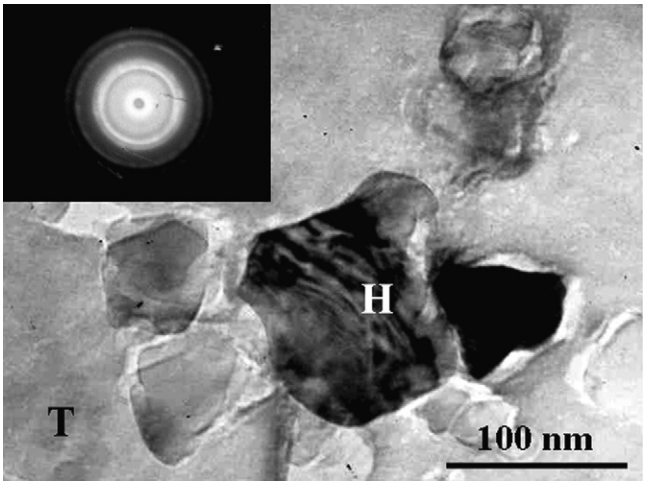

Fig. 2. Bright field (BF) TEM image and selected area diffraction pattern (SADP) of Ti with 5 A/cm^2-cathodic pretreatment.

SADP taken from an area that covers fine titanium hydrides (H) and titanium matrix (T). The diffraction spots are obtained from the titanium matrix (not shown). Diffraction ring patterns from titanium hydrides reveal that the titanium matrix is an ordered structure and that titanium hydride is polycrystalline. The titanium hydride is a nanostructure. The microstructures of the Ti with cathodization were dual phases (titanium and titanium hydride). Fine titanium hydride was formed by hydrogen charging. TEM micrographs and selected area diffraction patterns of pure Ti and the Ti with anodization at various cathodic current densities were also obtained. The TEM micrograph clearly demonstrates sharp diffraction spots in the diffraction patterns of the machined Ti, revealing that the machined Ti was crystalline. The grain size of the Ti was slightly smaller after undergoing 0.1 A/cm^2 hydrogen-charged treatment and the average grain size was 50 nm. Diffused rings dominate the electron diffraction patterns of the 1 A/cm^2 hydrogen-charged Ti, indicating that the Ti–O film was polycrystalline. Moreover, the grain size of the TiO_2 film with 5 A/cm^2 hydrogen-charged treatment was only ~5 nm, revealing that not only was the nanophase TiH_2 formed during cathodization, but also nanocrystallization was caused by the hydrogen reactions and the dissolution of titanium hydrides during anodization.

Fig. 3 displays the O 1s spectra of Ti with various cathodic pretreatments. Ti reacted with O as the current densities increased, indicating that titanium oxide compounds were present on the Ti surface. Huang et al. obtained similar results. The valence states of Ti^{4+} and Ti^{3+} were located at the surface, indicating that a definite O cavity was present under the surface [9]. Therefore, the grain size declined and the TiO_2 compound was formed as the duration of electrochemical treatment increased.

Fig. 4 presents depth profiles of TiO_2/Ti following anodization and anodization with cathodic pretreatment, respectively. The thickness of oxide layer on an anodized-Ti and a hydrogen-charged Ti were further examined by oxygen depth profiles, as shown in Fig. 4(a–b). The concentration of oxygen was observed to be high on the treated surface. Moreover, O diffuses toward the Ti surface after electrochemical treatment, indicating the formation of a titanium oxide layer. The thicknesses of Ti with anodization and with anodization with cathodic pretreatment are 200 and 330 nm, respectively. It is evident that bone-implant contact and bone volume were higher for Ti implants with electrochemical treatments than for pure Ti implants [10,11]. It reveals that a high degree of bone contact and bone formation are achieved with titanium implants which are modified with respect to oxide thickness.

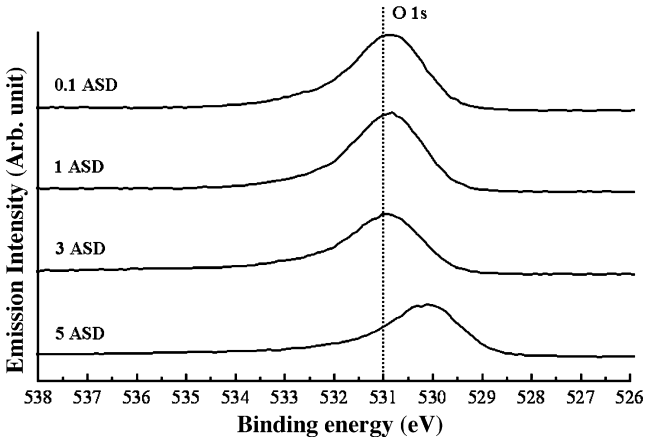

Fig. 3. O 1s spectra of Ti with cathodic pretreatment at various current densities.

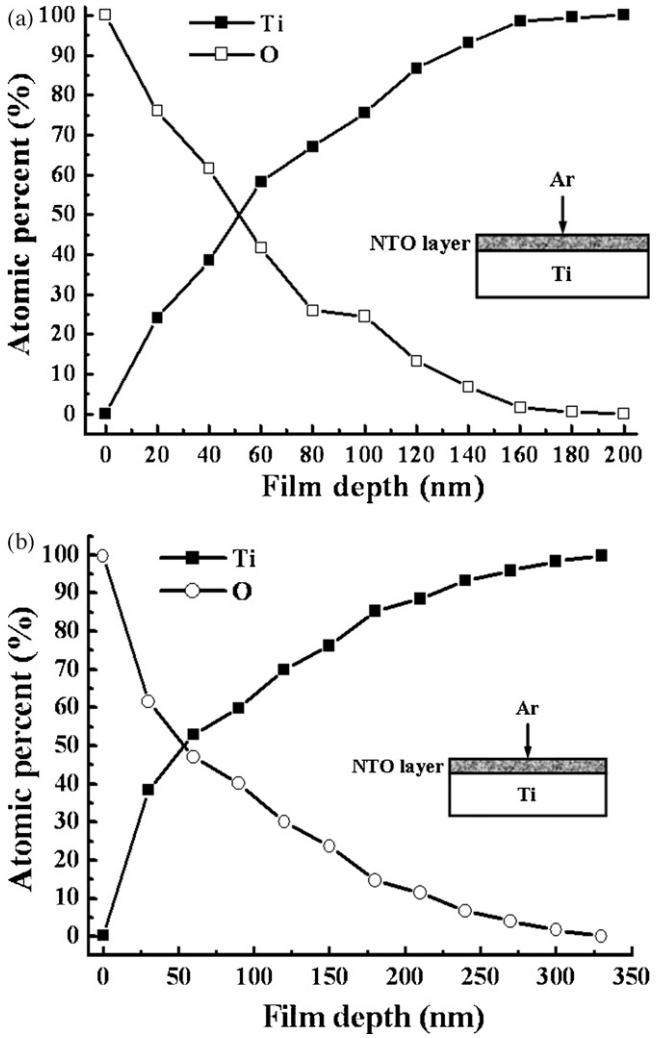

Fig. 4. XPS depth profiles of Ti with: (a) 15 A/cm^2-anodization and (b) 15 A/cm^2-anodization with 5 A/cm^2-cathodic pretreatments.

Fig. 5 displays the surface morphologies of the titanium with electrochemical treatments. Fig. 5(a) presents the surface morphology of Ti after anodization at a current density of 15 A/cm^2. The microporosity is obvious. Nanoporous structures were observed on the surface, when the current density of cathodic pretreatment was between 0.1 and 5 A/cm^2. A nanoporous Ti surface was obtained after the Ti was treated at 15 A/cm^2 for anodization with cathodic pretreatment at 5 A/cm^2, as shown in Fig. 5(b). A microporous structure is typically obtained by immersion in NaOH solution at high temperature for a long period [11–15]. A multi-nanoporous structure and a thicker titanium oxide layer were observed following anodization with cathodic pretreatments. As is widely believed, the

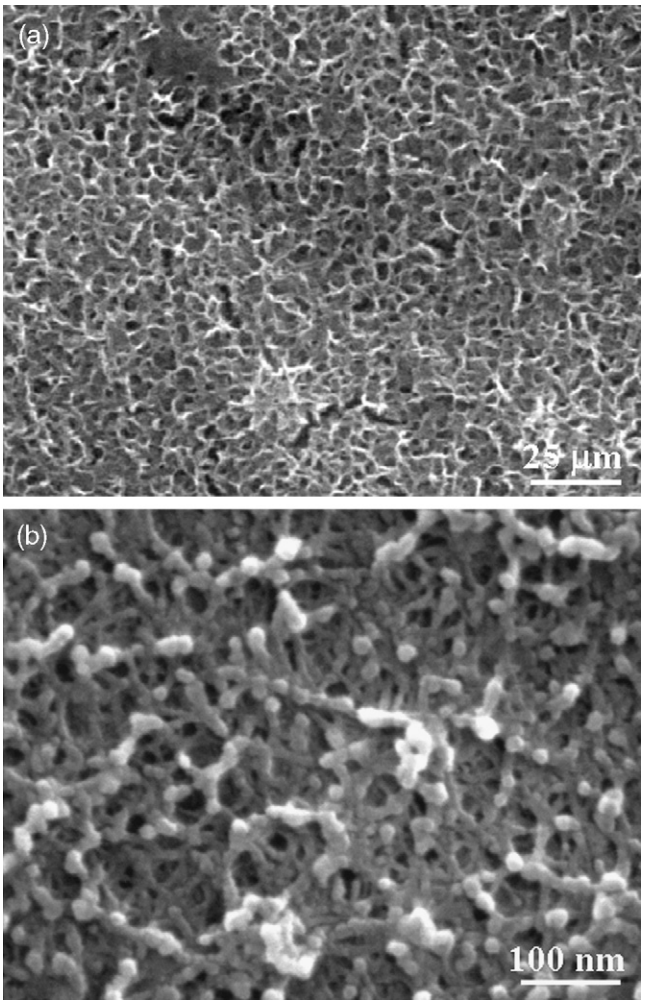

Fig. 5. Surface morphology of Ti with: (a) 15 A/cm^2-anodization and (b) 15 A/cm^2-anodization with 5 A/cm^2-cathodic pretreatments.

biocompatible improvement of implants is attributable to the thicker oxide layer and porosity, which enhances the adhesion between artificial bone and genuine bone [18].

Based on the above investigation, the formation mechanisms of porous TiO_2 on Ti sheets with and without treatments were discussed clearly as follows: Ti sheets undergo a hydrogen absorption reaction. The hydrogen was present on their surfaces. The depth of penetration of hydrogen was limited to the vicinity of the surface (1–5 nm) and the amount of hydrogen was extremely low (ppm). Hydrogen is present because of penetration into the interior during mechanical polishing or chemical etching in the mixture of HF and HNO_3 [7,8,22]. The amount of hydrogen is too low to form a large amount of the nano-TiH_2 phase [8]. Accordingly, the surface does not have a porous structure, and native titanium oxide is thin (1–5 nm). The barrier capability of TiO_2 films against metal ions diffusion can be improved by incorporating oxygen into the Ti surface and increasing the thickness of the oxide using surface treatment. Adding impurities, such as N and O, and increasing the thickness of the oxide have been reported to improve the properties of TiO_2 [16,17]. Increasing the thickness of the titanium oxide layer on Ti increased the albumin/fibrinogen adsorption ratio by a factor of six [18]. Doping Ti_2O_5 into TiO_2 ceramics has also been reported to improve the biocompatibility of the material [19]. The TiO_2 layer formed by anodic treatment has a thick oxide layer with a thickness of ~140 nm and a microporous structure. The oxide growth behaviors appear to have reduced the anodic forming voltage in acetic acid and sodium hydroxide by increasing the electrolyte temperature. The redox reaction was exothermic. Anodization involves a change of enthalpy of $\Delta H > 0$ in the system. Therefore, increasing the temperature favors the reactants as the temperature of the electrolyte rises. Hence, increasing the temperature of the electrolyte inhibits the formation of the oxide film because the thickness of the anodic oxide film is generally limited to less than 200 nm [20]. The redox reaction dominates the formation of the oxide layer, and the penetration and reaction of hydrogen result in the formation of microporous structures. Furthermore, the absorbed hydrogen and cathodization may induce the formation of TiH_2. As the TiH_2 is produced on the surface, it is dissolved by anodization and formed nanopores. Even though the Ti surface was initially covered with native oxides, the TiH_2 layer was formed after cathodic treatment in sulfuric acid. Anodizing treatment can form a TiO_2 layer with a nanoporous network. The formation and dissolution of nano-TiH_2 are believed to be related to the thickness of the TiO_2 layer formed by anodization. This fact explains why the thickness of the TiO_2 layer obtained by anodization without cathodic pretreatment is just half of that obtained with cathodic pretreatment. A porous layer is reportedly obtained at a high temperature during a long duration [7,8,12,21]. Hydrogen must be absorbed or nano-TiH_2 formed to generate the nanoporous TiO_2 layer during anodization treatment with cathodic pretreatment. The nanophases and nanocrystallization dominate the formation of the nanoporous network and the amorphous-like TiO_2 layer. A highly biocompatible TiO_2/Ti implant produced under such conditions.

4. Conclusion

This investigation examined the effectiveness of titanium hydride as a sacrificial barrier on titanium. Nanostructural effects and oxidation were observed because of the phase transformations and the dissolution reactions of nanophase titanium hydride. The structure of the TiO_2 layer changed from polycrystalline to amorphous-like. Moreover, a multi-nanoporous layer was found on the titanium after anodization with cathodic pretreatments. The thickness of the TiO_2 layer was 330 nm. TiO_2/Ti sheets after anodization with cathodic pretreatment are thicker and more porous than as-machined Ti, cathodic Ti and anodic Ti sheets. The TiH_2 is important in forming multi-nanoporous TiO_2 layers. Cathodization involved the hydrogen evolution on both titanium and the hydrogen-charged titanium. Anodization was applied to dissolve nano-TiH_2 and form a thicker nanoporous TiO_2 layer. We believe that the presence of the TiH_2 phase on titanium is critical to preparing a multi-nanoporous TiO_2 layer.

Acknowledgements

The authors would like to thank the National Science Council of Republic of China for financially supporting this research under contract no. NSC-93-2320-B-038-034, NSC93-2314-B-038-038 and supporting partly by Wan-Fang Hospital, Taipei Medical University under contract no. 94TMU-WFH-202.

References

[1] S.L. Carlson, T.R. Rostlunt, B. Abrektsson, T. Abrektsson, P.I. Brånemark, Acta Orthop. Scand. 57 (1986) 285.
[2] B. Kasemo, J. Prosthet. Dent. 49 (1983) 832.
[3] R.J. Solar, S.R. Pollack, E. Korostoff, J. Biomed. Mater. Res. 13 (1979) 217.
[4] B. Friberg, K. Grondahl, U. Lekholm, P.I. Brånemark, Clin. Implant Dent. Relat. Res. 2 (2000) 184.
[5] B. Kasemo, J. Lausmaa, Sweden Dent. J. 28 (1983) 19.
[6] H.M. Kim, T. Kokubo, S. Fujibayashi, S. Nishiguchi, T. Nakamura, J. Biomed. Mater. Res. 52 (2000) 553.
[7] S.I. Tanaka, M. Aonuma, N. Hirose, T. Tanakib, J. Electrochem. Soc. 149 (2002) D167.
[8] S.I. Tanaka, M. Aonuma, N. Hirose, T. Tanakib, J. Electrochem. Soc. 149 (2002) F186.
[9] N. Huang, P. Yang, X. Cheng, Y. Leng, X. Zheng, G. Gai, Z. Zhen, F. Zhang, Y. Chen, X. Liu, T. Xi, Biomaterials 19 (1998) 771.
[10] Y.T. Sul, C.B. Johansson, Y. Jeong, A. Wennerberg, T. Albrektsson, Clin. Oral. Impl. Res. 13 (2002) 252.
[11] B. Feng, J.Y. Chen, S.K. Qi, L. He, J.Z. Zhao, X.D. Zhang, J. Mater. Sci. Mater. Med. 13 (2002) 457.
[12] H.H. Kim, F. Miyaji, T. Kokubo, S. Nishiguchi, T. Nakamura, J. Biomed. Mater. Res. 5 (1999) 100.
[13] M. Takemoto, S. Fujibayashi, M. Neo, J. Suzuki, T. Kokubo, T. Nakamura, Biomaterials 26 (2005) 6014.
[14] H.B. Wen, Q. Liu, J.R. De Wijn, K. De Groot, F.Z. Cui, J. Mater. Sci. Mater. Med. 9 (1998) 121.
[15] S. Fujibayashi, T. Nakamura, S. Nishiguchi, J. Tamura, M. Uchida, H.M. Kim, T. Kokubo, J. Biomed. Mater. Res. 56 (2001) 562.
[16] B. Kasemo, J. Lausmaa, Environ. Health. Perspect. 5 (1994) 41.
[17] J.R. Goldberg, J.L. Gilbert, Biomaterials 25 (2004) 851.
[18] Y.T. Sul, C.B. Johansson, Y. Jeong, T. Albrektsson, Med. Eng. Phys. 23 (2001) 329.
[19] H.M. Kim, F. Miyaji, T. Kokubo, T. Nakamura, J. Mater. Sci. Mater. Med. 8 (1997) 341.
[20] M.C. Sunny, C.P. Sharma, J. Mater. Appl. 5 (6) (1991) 89.
[21] R. Ebert, M. Schaldach, World Congress on Medical Physics and Biomedical Engineering, vol. 3, Hamburg, (1982), p. 7.
[22] Y.M. Yeh, C.S. Chen, M.H. Tsai, Y.C. Shyng, S.Y. Lee, K.L. Ou, J. Appl. Phy. 44 (2) (2005) 1086.